# The geothermal gradient shapes microbial diversity and processes in natural gas-bearing sedimentary aquifers

Taiki Katayama[1], Hideyoshi Yoshioka[1], Toshiro Yamanaka[2], Susumu Sakata[1] and Yasuaki Hanamura[3]

[1]Institute for Geo-Resources and Environment, Geological Survey of Japan (GSJ), National Institute of Advanced Industrial Science and Technology (AIST), Ibaraki 305-8567, Japan.
[2]School of Marine Resources and Environmental Sciences, Tokyo University of Marine Science and Technology, Tokyo 108-8477, Japan.
[3]JX Nippon Oil and Gas Exploration Corporation, Tokyo 100-8163, Japan.

*Correspondence to*: Taiki Katayama (katayama.t@aist.go.jp)

**Abstract.** Deep subsurface microorganisms constitute over 80% of Earth's prokaryotic biomass and play an important role in global biogeochemical cycles. Geochemical processes driven by geothermal heating are key factors influencing their biomass and activities, yet their full breadth remains uncaptured. Here, we investigated the microbial community composition and metabolism in microbial natural gas-bearing aquifers at temperatures ranging from 38 °C to 81 °C, situated above nonmicrobial gas and oil-bearing sediments at temperatures exceeding 90 °C. Cultivation-based and molecular gene analyses, including radiotracer measurements, of formation water indicated variations in predominant methanogenic pathways across different temperature regimes of upper aquifers: high potential for hydrogenotrophic/methylotrophic, hydrogenotrophic and acetoclastic methanogenesis at temperatures of 38 °C, 51−65 °C and 73−81 °C, respectively. The potential for acetoclastic methanogenesis correlated with elevated acetate concentrations with increasing depth, possibly due to the decomposition of sedimentary organic matter. In addition to acetoclastic methanogenesis, in aquifers at temperatures as high or higher than 65 °C, acetate is potentially utilized by microorganisms responsible for the dissimilatory reduction of sulfur compounds other than sulfate because of their high relative abundance at greater depths. The stable sulfur isotopic analysis of sulfur compounds in water and oil samples suggested that hydrogen sulfide, generated through the thermal decomposition of sulfur compounds in oil, migrates upward and is subsequently oxidized with iron oxides present in sediments, yielding elemental sulfur and thiosulfate. These compounds are consumed by sulfur-reducing microorganisms, possibly reflecting elevated microbial populations in aquifers at temperatures as high or higher than 73 °C. These findings reveal previously overlooked geothermal heat-driven geochemical and microbiological processes involved in carbon and sulfur cycling in the deep sedimentary biosphere.

## 1 Introduction

The deep subsurface environment harbors a substantial fraction of Earth's prokaryotes (Mcmahon and Parnell, 2014; Magnabosco et al., 2018), constituting over 80% of the total prokaryotic biomass (Bar-On et al., 2018). The metabolic activities of these microorganisms play a pivotal role in global biogeochemical cycling, such as carbon, nitrogen and sulfur (Magnabosco

et al., 2018; Aloisi et al., 2006). A prominent example is methane production. Much of the methane hydrate, the largest methane reservoir on Earth, is suggested to be generated by these subsurface microorganisms (Kvenvolden, 1995). Additionally, coalbed methane and shale gas reservoirs also may contain a significant amount of microbially-derived methane (Vinson et al., 2017).

35      In the absence of light energy, microorganisms inhibiting deep sedimentary environments rely on chemical energy derived from the oxidation of reduced substances in sediments with organic matter oxidation being particularly critical (Lovley and Chapelle, 1995; Jørgensen and Boetius, 2007; Arndt et al., 2013). The labile components are consumed during burial, limiting the availability of energy sources for microorganisms as sediment age increases (Middelburg, 1989). However, substantial populations of active microbial cells have been observed even in deep buried sediments older than 16 million yr

40      (Schippers et al., 2005). It has been hypothesized that temperature increase during burial stimulates thermal or biological degradation of recalcitrant organic matter, possibly sustaining microbial activities (Parkes et al., 2000). To address the fundamental questions of how microbial cells in the deep biosphere can survive with limited energy sources, this hypothesis has been examined through numerical simulations (Horsfield et al., 2006), laboratory incubation experiments (Parkes et al., 2007), and geochemical analysis (Malinverno and Martinez, 2015) of subseafloor sediments. Thus, while temperature increase

45      during burial is posited to drive subsurface microbial activity, field observation-based microbiological research remains limited, and the mechanisms are not fully understood.

      As sediment compaction progresses with burial, pore size and permeability decrease, reducing the living space, available water, and nutrients, thereby inhibiting microbial growth (Fredrickson et al., 1997). To investigate the impact of temperature increase on subsurface microbial ecosystem, it is essential to target subsurface environments where these inhibitory factors are

50      minimized. Therefore, we focused on aquifers, which, even at great depths, maintain high porosity and permeability, providing ample living space and water for microorganisms (Fredrickson et al., 1997; Mcmahon and Chapelle, 1991; Lovley and Chapelle, 1995; Krumholz et al., 1997).

      In this study, we targeted a gas field in central Japan, where aquifers exhibit a wide temperature range, spanning approximately 35 to 80 °C, due to a steep geothermal gradient (5 °C per 100 m) (Kato, 2018). We collected formation water

55      (FW) from each aquifer and employed a comprehensive approach, including geochemical analysis, radiotracer measurements, molecular gene analysis and cultivation experiments to evaluate microbial diversity, community structure, and potential metabolic processes. Furthermore, in this field, high-temperature oil deposits situated deeper than the series of aquifers. We, therefore, also examined the impact of oil components on microorganisms in the upper aquifers. The aim of this study is to elucidate the effects of temperature rise and associated geochemical processes, such as the decomposition of sedimentary

60      organic matter and petroleum formation, on microbial diversity, community structure, and metabolic processes, including the conversion of carbon and sulfur compounds.

## 2 Materials and Methods

### 2.1 Site description and sample collection

The study site was located along the Japan Sea coast in Tainai city, Niigata Prefecture, Japan (Fig. 1a). The reservoirs are distributed in the Neogene and Quaternary formations of the Niigata sedimentary basin. The reservoirs of dissolved natural gases are distributed within the Pliocene to Pleistocene Nishiyama and Pleistocene Haizume Formations and mainly consist of sandstone or conglomerate (Kobayashi, 2000; Fukano et al., 2023). These sediments are interpreted as turbidite sediments deposited under submarine fan to shelf conditions (Takano et al., 2001). Logging analysis of the gas production wells revealed that each reservoir layer was separated by silt-mudstone, and their horizontal continuity was confirmed. Oil and associated gas are deposited along anticlinal structures in the lower part of the Nishiyama Formation and the Pliocene Shiiya Formation (Fukano et al., 2023). The reservoirs of oil deposits consist of sandstone in turbidite sediments deposited under submarine fan and shelf conditions (Takano et al., 2001). The chemical and isotopic compositions of natural gases (Kaneko and Igari, 2020) indicate that methane dissolved in upper aquifers is primarily of microbial origin, whereas that from lower oil deposits primarily originates from oil-associated thermogenic processes (Fig. S1) based on the classification by Milkov and Etiope (Milkov and Etiope, 2018). In this gas field, gases are dissolved in FW and produced for commercial purposes by pumping gas-associated FW from upper aquifers. Crude oil and gases are also collected from lower oil deposits.

The FW samples subjected to microbiological analyses were collected from the separate reservoir layers in the Haizume and Nishiyama Formations through 6 commercial production wells with depths ranging from approximately 500 to 1430 mbgs (Fig. 1a, b). Crude oil and associated FW samples were collected from the Shiiya Formation through tanks separating oil, FW and gas produced from multiple wells and used for microbial cell counting and geochemical analysis. The geological information and analytical purpose of each sample are summarized in Table S1.
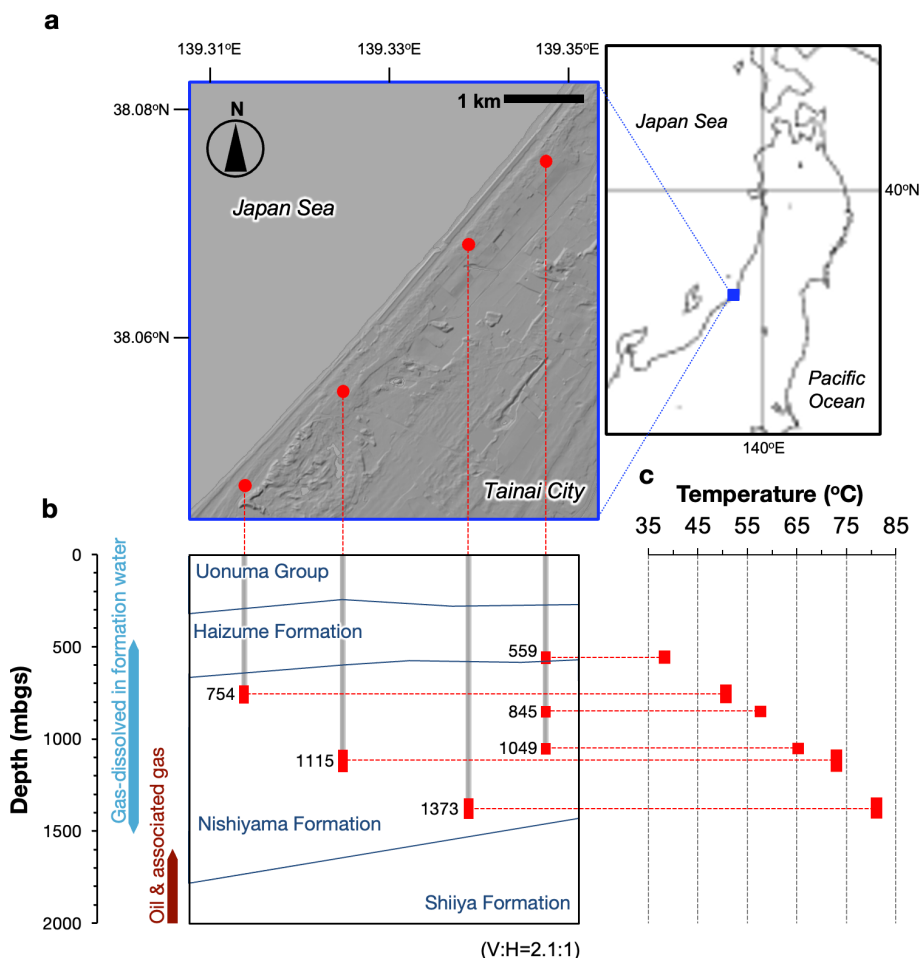
**Fig. 1.** Geological map of the study site (a), and the relationship between the depths of the wells from which water samples were taken for microbiological analyses (b) and the measured water temperatures (c). The ratio of the vertical to horizontal scale of the cross section is 2.1:1 (b). The range of the well strainers is indicated by a red bar (b, c), and the average depth (mbgs) of each well strainer is also indicated (b). Because three wells are present at the same location, only one well is shown in panel b.

FW samples for methanogen activity measurements and cultivation were collected in sterilized glass bottles with butyl rubber stoppers and screw caps. The bottles were purged with $N_2$ gas before and during sample collection and then filled with FW to prevent the penetration of air. For the molecular analysis, 2-L FW samples were collected and filtered through a 0.2-μm pore size Millipore Express Plus membrane filter (Millipore, Billerica, MA, USA) to harvest microbial cells, which were subsequently stored at -20 °C. The samples used for total cell counts were fixed with formalin at a final concentration of 2% (v/v) immediately after sampling and stored at 4 °C. Zinc acetate solution (2.0 M) was added to the water sample to fix the

hydrogen sulfide dissolved in the FW immediately after collection, and the solution was used for the measurement of the hydrogen sulfide concentration.

## 2.2 Geochemical analysis

100 The inorganic chemical and total organic carbon contents in the FW samples were measured as described previously (Katayama et al. 2015), and the analytical methods used for each compound are summarized in Table S2. The concentrations of formate, acetate, propionate and butyrate were measured using a Prominence HPLC system (Shimadzu Co. Ltd., Kyoto, Japan) equipped with an electrical conductivity detector. The concentration of the fixed hydrogen sulfide sample was measured colorimetrically with a SmartSpecTM Plus spectrophotometer (Bio-Rad, CA, USA) using ferrous hydrogen sulfide reagents

105 (HACH, Loveland, CO, USA). Hydrocarbon components in FW samples from upper aquifers were extracted and concentrated with dichloromethane and qualitatively analyzed using gas chromatography–mass spectrometry (5973 GC–MS, Agilent Technologies, CA). The crude oil sample from the oil deposits was diluted with hexane and qualitatively analyzed via GC–MS. The concentration of phenols in the FW sample was measured via the 4-aminoantipyrine spectrophotometric method. The concentrations of methanol, toluene and xylene in the FW sample were measured using a GC–MS (Agilent 5973, Agilent

110 Technologies) instrument equipped with a headspace sampler (Agilent 7697A, Agilent Technologies). The number of replication and the standard deviation value for each measurement are provided in Table S3.

The stable oxygen and hydrogen isotopic compositions of the FW samples were measured via wavelength-scanned cavity ring-down spectroscopy (WS-CRDS) via a laser spectroscopy analyzer (Picarro L2120-i). Each isotopic ratio was measured 6 times per sample, with the standard deviations of $\delta D$ and $\delta^{18}O$ less than 2.0‰ and 0.5‰, respectively.

115 Stable sulfur isotope analysis of sulfate and hydrogen sulfide dissolved in FW was performed as described previously (Yamanaka et al., 2013; Katayama et al., 2019). For stable isotope analysis of elemental sulfur (dissolved in FW), hydrogen sulfide dissolved in FW samples was first removed by precipitation using zinc acetate solution, followed by filtration using filter paper to trap the generated zinc sulfide. Liquid–liquid extraction of elemental sulfur was performed from the filtrate with carbon disulfide followed by evaporation of carbon disulfide in a sand bath (~60 °C), and crystallized elemental sulfur was

120 measured by an elemental analyzer/isotope ratio mass spectrometer (IsoPrime EA; GV Instruments, Manchester, UK). For stable sulfur isotope analysis of sulfur compounds in oil, the compounds were oxidized and decomposed in a high-pressure oxygen combustion unit (Parr Bomb), precipitated as barium sulfate, wrapped in a tin capsule containing $V_2O_5$, and measured using the elemental analyzer/isotope ratio mass spectrometer. Each sulfur isotope ratio represents the average of duplicate measurements, with deviations less than 0.4‰.

125

## 2.3 Methanogenic activity measurement using a radiotracer

The methane production rates in the FW samples were measured using radiotracer experiments as described previously (Katayama et al., 2015). Briefly, a 20 ml water sample in a 50 ml serum vial sealed with a butyl rubber stopper and aluminum crimp was injected with one of the radiotracers: $^{14}C$-bicarbonate (10 ml, 199 kBq), [$2$-$^{14}C$]-acetate (10 ml, 81 kBq) or $^{14}C$-

methanol. The vials were incubated under an atmosphere of $N_2/CO_2$ (80:20, v/v) for 14, 28 or 42 days. The activity measurements were conducted in triplicate for each of the three cultivation periods and for each of the three radiotracers. The incubation temperatures were set close to the measured water temperature of each sample (i.e., 559 mbgs, 37 °C; 754 mbgs, 50 °C; 845 mbgs, 55 °C; 1049 mbgs, 65 °C; 1115 mbgs, 75 °C; 1373 mbgs, 80 °C). The produced $^{14}CH_4$ was oxidized to $^{14}CO_2$ and measured using a Tri-Carb 3100TR liquid scintillation counter (Perkin Elmer). The $^{14}C$ activity at time zero was used as a control. The methane production rate was calculated using the equation $ap/(art)C$, where $ap$ and $ar$ are the activities of the product and added reactant, respectively; $t$ is the incubation period; and C is the *in situ* concentration of the reactant.

### 2.4 Direct cell counts

Twenty milliliters of formation water sample was filtered through a 0.2-μm-pore-size Isopore membrane filter (Millipore), stained with SYBR Green solution (10 μg ml$^{-1}$) for 10 minutes, and observed under an epifluorescence microscope (BX51; Olympus, Tokyo, Japan). The detection limit for cell abundance was $4.3 \times 10^2$ cells ml$^{-1}$.

### 2.5 Quantitative PCR

DNA was extracted from the membrane filter filtered through formation water samples using a PowerWater kit (MoBio Laboratories, CA, USA) according to the manufacturer's protocol. Quantitative PCR targeting bacterial and archaeal 16S rRNA genes and the *mcrA* gene (encoding a methyl-coenzyme M reductase alpha subunit) in formation water samples was performed as described previously (Katayama et al., 2016).

### 2.6 Sequencing of the 16S rRNA and mcrA genes

The 16S rRNA genes (including variable regions 4 and 5) were amplified and sequenced as described previously (Katayama et al., 2016). In brief, the primers Univ515F (5'-GTGYCAGCMGCCGCGGTA) and Univ926R (5'-CCGYCAATTCMTTTRAGTT) were used for PCR amplification. Amplicons were sequenced on an Illumina MiSeq platform (Illumina, Inc., San Diego, CA, USA) using a 250 bp paired-end protocol at the J-Bio21 Center, Nippon Steel and Sumikin Eco-Tech Corporation (Tsukuba, Japan).

The *mcrA* genes were amplified, cloned and sequenced from the FW and methanogen culture samples (as described below) as described previously (Katayama et al., 2016) with the following modifications. The primers MLf and MLr (Luton et al., 2002) were used for PCR amplification, and clones were subjected to Sanger sequencing using Eurofin Sanger sequencing services (Tokyo, Japan).

### 2.7 Sequence analysis

The 16S rRNA gene amplicon reads were analyzed using the Fastx toolkit (ver 0.0.14) and QIIME 2 (ver 2022.2). The quality-filtered sequences with an average length of 375 bp were clustered as amplicon sequence variants (ASVs) based on the DADA2

algorithm and classified using a Bayesian classifier based on the Silva taxonomy SSU Ref 138.1 dataset (Pruesse et al., 2007) with a confidence threshold of 80%. In this study, the nomenclature of prokaryotic lineages was based on this SILVA taxonomy.

165      Sanger sequences of the *mcrA* genes derived from the FW and culture samples were aligned using MAFFT version 7 (Katoh and Standley, 2013). Nucleotide sequences with >85% sequence identity were treated as operational taxonomic units (OTUs) according to the cutoff values estimated by Yang et al. (Yang et al., 2014). For each OTU, the most abundant sequence was selected as the representative sequence, which was translated to amino acids *in silico* and then searched against BLAST (http://blast.ncbi.nlm.nih.gov/Blast.cgi).

170      The 16S rRNA gene amplicon data were submitted to the DDBJ Sequence Read Archive database under accession number PRJDB16863. The GenBank/EMBL/DDBJ accession numbers for the *mcrA* gene sequences are LC783983-LC783991.

### 2.8 Cultivation of methanogens

The basal media used for the methanogenic cultures consisted of 10 mM $NH_4Cl$, 1 mM $KH_2PO_4$, 15 mM $MgCl_2 \cdot 6H_2O$, 350

175 mM NaCl, 1 mM $CaCl_2 \cdot 2H_2O$, 30 mM $NaHCO_3$, 1 ml $l^{-1}$ selenium and tungsten solution, 1 ml $l^{-1}$ trace element solution, 1 ml $l^{-1}$ vitamin solution, 1 ml $l^{-1}$ resazurin solution (1 mg $ml^{-1}$), and 0.1 mM titanium(III) citrate (as a reducing agent) (Katayama et al., 2020). Using an anaerobic chamber, 40 ml of the FW sample was mixed with 20 ml of this saline mineral medium and then dispensed into 110-mL serum vials. The vials were sealed with butyl rubber septa and aluminum crimps under an atmosphere of $N_2/CO_2$ (80:20, v/v; 0.1 MPa). The culture was supplemented with either $H_2/CO_2$ (80:20, v/v; 0.1 MPa) plus

180 formate (20 mM) plus yeast extract (0.02%) (for culturing hydrogenotrophic methanogens), acetate (20 mM) (for culturing acetoclastic methanogens) or methanol (10 mM) plus trimethylamine (10 mM) (for culturing methylotrophic methanogens). The incubation temperatures were set at a value close to the measured water temperature of each sample (as described for the radiotracer measurement methods). Methane production was measured using a GC equipped with a TCD. After methane production was terminated, 4 mL of the enrichment cultures were harvested by centrifugation, and *mcrA* gene sequencing

185 analysis was conducted as described above.

## 3 Results

### 3.1 Geochemistry of the formation water

The geochemical properties of the FW samples are summarized in Table S1 and S3. The water temperatures ranged from 38 °C

190 to 81°C in the FW samples from upper aquifers (Fig.1c) and from 67 to 96 °C in the samples from lower oil deposits (Table S1). The FW from the upper aquifers was characterized by higher concentrations of bicarbonate and ammonium ions, comparable concentrations of chloride and sodium ions, and almost no sulfate in comparison with present-day seawater (Table S3). The depletion of electron acceptors for microbes, such as nitrate, nitrite and sulfate, resulted in a low redox potential of FW lower than -180 mV.

195    The crude oil sample from the lower oil deposits contained n-alkanes with carbon numbers of 9-35, whereas such alkanes were not detected in the FW samples from the upper aquifers (Fig. S2). On the other hand, volatile hydrocarbons such as toluene and xylene were detected in the FW samples from the upper aquifers and were most likely derived from oil. In the 1049 and 1115 mbgs samples, elemental sulfur was also detected. The concentrations of phenols dissolved in the FW samples increased from 1115 mbgs to greater depths (above >73 °C), whereas toluene or xylene did not (Table S3). Similar increasing

200    trends at greater depths were also observed for formate, acetate, propionate and total organic carbon. A steep increase in acetate concentration at >70 °C has also previously been observed in deep subseafloor sediments (Heuer et al., 2020; Parkes et al., 2007), possibly due to the decomposition of sedimentary organic matter along with elevated geothermal heating (Parkes et al., 2007). Considering that phenols are prominent pyrolysis products of terrestrial kerogens according to previous studies  (Larter and Senftle, 1985; Van De Meent et al., 1980), it is conceivable that the presence of these compounds is also due to the

205    decomposition of sedimentary organic matter associated with geothermal heating.

**3.2 Stable isotopic analysis of sulfur compounds**

Fig. 2 illustrates the depth distribution of stable sulfur isotope ratios in different sulfur species, namely, sulfide, elemental sulfur and sulfate in FW and sulfur compounds in oil. Elemental sulfur exhibited the lowest $\delta^{34}$S (-3.3 − -2.0‰), followed by

210    hydrogen sulfide (+1.5 − +9.4‰), sulfur compounds in oil (+8.6 − +9.6‰), and sulfate (+12.1 − +19.4‰). Differences in $\delta^{34}$S values were not clearly observed between samples from upper aquifers and lower oil deposits for each sulfur species.
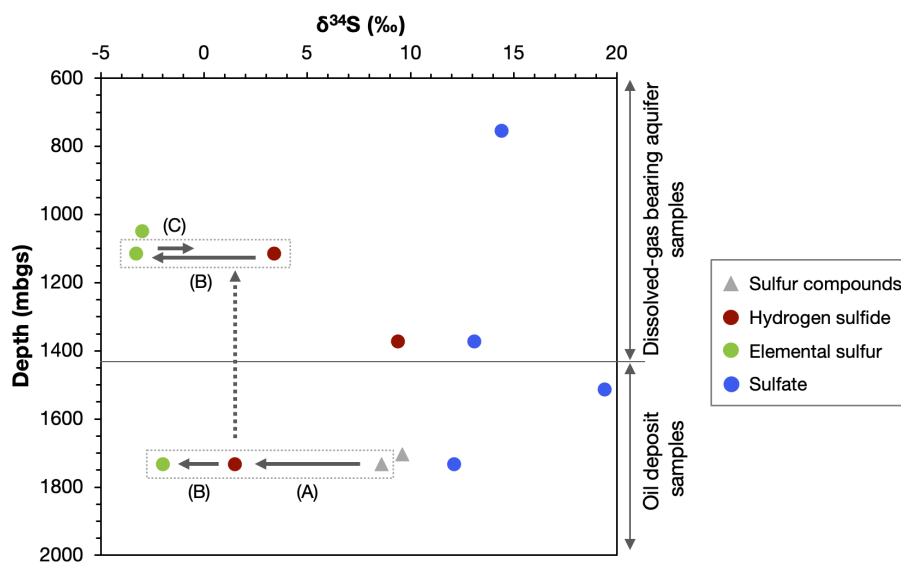
**Fig. 2.** Depth distribution of stable sulfur isotopic ratios in sulfur species in the formation water (FW, circle) and oil (triangle) samples. The arrows indicate the possible changes in the ratios due to isotopic fractionation associated with the following

215    reactions: thermal decomposition of oil sulfur to hydrogen sulfide (A), oxidation of upward migrated hydrogen sulfide (broken

arrow) with iron oxides to elemental sulfur (B) and biological dissimilatory reduction of elemental sulfur to hydrogen sulfide (C; for details, see the Discussion section).

### 3.3 Hydrogen and oxygen isotope ratios of the formation water samples

To assess the potential mixing of formation water (FW) from upper aquifers and lower oil deposits, isotopic values ($\delta^{18}$O and $\delta$D) of water samples collected from specific layers were determined. In the $\delta^{18}$O-$H_2O$ vs. $\delta$D-$H_2O$ diagram (Fig. S3), FW samples collected from aquifers above 1115 mbgs plot along the meteoric water line in this region (Kato and Kajiwara, 1986; Waseda and Nakai, 1983). In addition, the chlorine ion concentration of the FW sample at the uppermost depth of the 554 mbgs sample was lower than that of the present seawater (Table S3), suggesting the mixing of surface water in this sample. In samples below 1373 mbgs, there was a trend of increasing $\delta^{18}$O-$H_2O$ concentration with increasing depth, possibly due to the isotopic exchange between formation water and sedimentary minerals at elevated temperatures (Clayton et al., 1966). The difference in water isotopic ratios, coupled with the presence of aquiclude silt-mudstone layers between (Takano et al. 2001), indicates no mixing of formation water between the upper aquifers and lower oil deposits.

### 3.4 Potential for methanogenic activity

The $^{14}$C tracer experiments detected the potential activity of methanogenesis from $CO_2$, acetate and methanol (hydrogenotrophic, acetoclastic and methylotrophic pathways, respectively) in all 6 FW samples from the dissolved natural gas-bearing aquifers (Fig. 3a). The depth-related patterns of the activity rates clearly differed among these three methanogenic pathways. Methylotrophic methanogenesis peaked at the shallowest sample (559 mbgs) and decreased by at least three orders of magnitude in deeper samples. The hydrogenotrophic methanogenic rates were greater in the three shallowest samples (< 845 mbgs) than in the deeper samples (> 1049 mbgs), and the maximum rates were observed in 845 mbgs. The activity rates of acetoclastic methanogenesis were at least two orders of magnitude greater in deeper samples (1115 and 1373 mbgs).
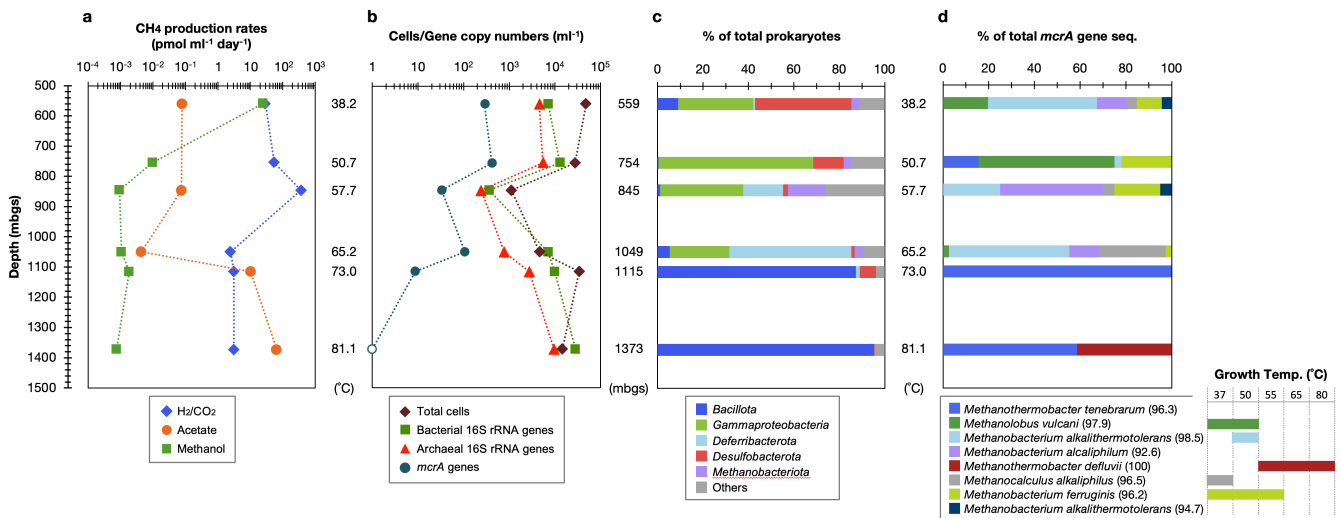
**Fig. 3.** Depth (temperature)-related changes in potential methanogenic activity (a), microbial population (b), and prokaryotic (c) and methanogen (d) community compositions based on the 16S rRNA (c) and *mcrA* (d) gene sequences in formation water samples from the upper aquifers. The growth temperatures (e) are expressed by the detection of *mcrA* gene sequences from both original formation water samples and methanogen cultures at different temperatures (for details, see Table S4).

### 3.5 Enumeration of total microbial cells and of the 16S rRNA and mcrA genes

The number of microbial cells in the FW samples ranged from $1.1 \times 10^3$ to $4.8 \times 10^4$ cells ml$^{-1}$ (Fig. 3b). The highest and lowest numbers were measured in the shallowest 559 and 845 mbgs samples, respectively. No microbial cells were observed in the oil-associated FW sample (1733 mbgs), in which water temperature was measured to be 96 °C (Table S3). Therefore, molecular gene sequencing analysis was not conducted on oil-associated FW samples from lower oil deposits.

The populations of bacteria, archaea and methanogens were measured via quantitative real-time PCR (Fig. 3b). The bacterial 16S rRNA gene copy numbers ranged from $10^2$-$10^4$ ml$^{-1}$, whereas those of archaea ranged from $10^2$-$10^3$ ml$^{-1}$. Bacterial and archaeal gene copy numbers were highest in the deepest sample (1373 mbgs). On the other hand, in this sample, the *mcrA* gene copy number was below the detection limits. The *mcrA* gene copy numbers tended to decrease with increasing depth.

### 3.6 Microbial community compositions

16S rRNA gene amplicon analysis was performed to examine the compositions of the prokaryotic and methanogenic communities. After quality filtering, the reads yielded 88,255-108,428 reads per sample. The major taxonomic groups (>10% of the total reads in at least one sample) were the phyla or classes *Bacillota* (formerly *Firmicutes*), *Gammaproteobacteria*, *Deferribacterota*, *Desulfobacterota* and *Methanobacteriota* (formerly *Euryarhcaeota*) (Fig. 3c). The members of *Bacillota* were abundant in two deeper samples (1115 and 1373 mbgs), accounting for >85% of the total sequences. In the shallower two samples (559 and 754 mbgs), *Gammaproteobacteria* and *Desulfobacterota* sequences were abundant, whereas *Gammaproteobacteria* and *Deferribacterota* sequences were abundant in the two intermediate depth samples (845 and 1049 mbgs). In the samples deeper than 1000 mbgs, only one ASV accounted for ≥50% of the total sequences in the sample. These genes were phylogenetically related to *Deferribacter desulfuricans* (100% sequence similarity, in the 1049 mbgs sample), *Thermacetogenium phaeum* (93% sequence similarity, in the 1115 mbgs sample) and *Thermanaeromonas toyohensis* (97% sequence similarity, in the 1373 mbgs sample). These species can commonly utilize sulfur compounds, such as thiosulfate and elemental sulfur, as electron acceptors and acetate as an electron donor (Takai et al., 2003; Hattori et al., 2000; Mori et al., 2002) Additionally, these genera are known to utilize a variety of electron acceptors: Deferribacter can use nitrate, iron (III), or manganese (Slobodkina et al., 2009); *Thermacetogenium* can use sulfate (Hattori et al., 2000); Thermanaeromonas can use nitrate, nitrite, sulfate, or fumarate (Gam et al., 2016).

The archaeal sequences accounted for 0.04-18.99% of the total sequence. The majority (>3% of the total archaea) were assigned to *Halobacterota*, *Methanobacteriota* and *Thermoplasmatota*, whereas the minor sequences were *Ca.* Asgardarchaeota, *Ca.* Hadarchaeota and *Nanobdellota* (formerly *Ca.* Nanoarchaeota). The sequences of hydrogenotrophic

methanogens, such as *Methanobacterium* and *Methanocalculus*, were abundant in shallower depth samples (<1050 mbgs), whereas *Archaeoglobaceae* were abundant in deeper samples (1115 and 1373 mbgs). Members of the *Archaeoglobaceae* family are known to reduce sulfur compounds (Liu et al., 2012). On the other hand, recent research has reported Mcr-dependent methanogenesis in *Archaeoglobaceae* from a hot spring (Buessecker et al., 2023). Based on this literature, acetate conversion to methane is possible through methanogenic pathways deduced from the reconstructed *Archaeoglobaceae* genomes (Buessecker et al., 2023). Other potential candidates for methanogens or hydrocarbon-oxidizing archaea known to possess the Mcr or Acr (alkyl-S-CoM reductase) gene in their genomes, such as *Ca*. Methanomethyliales, *Ca*. Nezhaarchaeales, *Ca*. Korarchaeia, *Ca*. Methanodesulfokores, *Ca*. Bathyarchaeia and *Ca*. Helarchaeales (Mei et al., 2023), were not detected in any of the samples.

### 3.7 Methanogen diversity in FW and culture samples based on the mcrA genes

A total of 29-46 clones per sample of the *mcrA* gene were grouped into 8 OTUs (Fig. 3d). Among these, 5 OTUs were also detected in the methanogenic cultures of the FW samples (Table S4). Similar to the results of the 16S rRNA gene sequencing analysis, methanogen diversity changed with depth. *Methanobacterium* and *Methanocalculus* were dominant in the samples from depths above 1050 mbgs, whereas only thermophilic *Methanothermobacter* was recovered in the deeper samples at 1115 and 1373 mbgs, resulting in an overall predominance of hydrogenotrophic methanogens throughout the depths. In 559 and 754 mbgs, the methylotrophic methanogen *Methanolobus* was also detected as a major proportion. Acetoclastic methanogens, such as *Methanosaeta* and *Methanosarcina*, were not detected in any of the samples. Additionally, unlike the results from the 16S rRNA gene sequencing analysis, *Archaeoglobaceae* were not detected in the samples from 1115 and 1373 mbgs. The absence of *mcrA* gene sequences for *Archaeoglobaceae*, which might participate in acetoclastic methanogenesis in these samples (as described above), highlights the bias and limitation of PCR-based *mcrA* gene sequencing analysis. This issue has been documented by Vítězová et al. (2021), who indicatied that *mcrA* gene analysis fails to detect specific methanogens, with their identification depending on the primers used. It could also explain the observed discrepancy between the highest ^{14}C acetoclastic activity and the lowest *mcrA* gene copy numbers at these high-temperature depths.

These depth-related distributions of methanogens were roughly correlated with their growth temperature, as observed in the enrichment cultures (Fig. 3d and 3e, Table S4). Methane production from $H_2$ and formate was observed in the enrichment cultures at depths from 37 to 80 °C, except at 70 °C, whereas no methane production was observed in acetate-amended cultures from any FW samples (data not shown). In cultures supplemented with methylated compounds, methane was detected only in 559 and 754 mbgs samples, i.e., at 37 and 50 °C, respectively.

### 4 Discussion

This study examined how microbial diversity and processes are shaped by geothermal heat and associated geochemical processes in deep subsurface environments, encompassing a range of temperatures from 38 °C to 81 °C. The geochemical and

hydrological analyses suggested the upward migration of volatile hydrocarbons derived from lower oil deposits to upper aquifers (Fig. S2 and Table S3), whereas no evidence indicated the mixing of water or less volatile n-alkanes between the upper aquifers and lower oil deposits (Fig. S2 and S3). Radiotracer measurements provided clear insight into the variations in potential methanogenesis across different temperature regimes (Fig. 3a). Molecular and cultivation experiments indicate that these variations align with the growth temperature ranges of major indigenous methanogens, except for high-temperature depths ($\geq$70 °C) (Fig. 3d). Our previous study also suggested that the upper temperature limit for growth in indigenous methanogens may reflect the potential for methanogenesis in deep subseafloor sediments (Katayama et al., 2022). The correlation between the high potential for acetoclastic methanogenesis and increased acetate concentration suggests that acetate generation, possibly driven by geothermal heating (Parkes et al., 2007), stimulates acetoclastic methanogenesis in high-temperature depths ($\geq$70 °C). Although syntrophic acetate oxidation (SAO) coupled with hydrogenotrophic methanogenesis is generally observed in high-temperature environments (Conrad, 2023), the potential for this SAO methanogenesis is unlikely at our study site. This inference is drawn from the observation that the levels of $^{14}$C-activity from acetate were as much as two orders of magnitude greater than those from carbonate in high-temperature depths ($\geq$70 °C). If SAO was the primary activity, the $^{14}$C activity from acetoclastic methanogenesis would be much lower than that from hydrogenotrophic methanogenesis. This is because $^{14}$C-CO$_2$ produced from $^{14}$C-acetate via SAO is diluted into the biocarbonate pool in the incubated FW sample, leading to the monitoring of $^{14}$C-CH$_4$ production from CO$_2$ with an extremely low level of $^{14}$C. We speculate that the predominant *Archaeoglobaceae* may play a role in converting $^{14}$C-acetate to $^{14}$C-methane at greater depths (1115 and 1373 mbgs).

In addition to driving the acetoclastic methanogenesis observed in the radiotracer experiments, elevated concentrations of acetate at greater depths (1115 and 1373 mbgs) may primarily serve for the dissimilatory reduction of sulfur compounds other than sulfate, such as elemental sulfur and thiosulfate. This is inferred from the high relative abundance of sulfur-reducing, rather than sulfate-reducing, microorganisms at those depths. This raises the question of how sulfur compounds are generated to sustain these sulfur-reducing microbes, possibly reflecting the relatively high microbial population at greater depths. Based on the sulfur isotopic analysis and previous literature, we suggest that elemental sulfur and/or thiosulfate are abiotically generated from sulfur compounds within crude oils according to the following reactions. Hydrogen sulfide can be generated through the thermal decomposition of sulfur compounds in crude oil (Zhu et al., 2017). The occurrence of this reaction is supported by the lower $\delta^{34}$S values of hydrogen sulfide in the FW sample from the lower oil deposits compared with those of sulfur compounds in oil [Fig. 2 (A)]. This generated hydrogen sulfide, together with other oil-derived volatile hydrocarbons, such as toluene and xylene, may migrate upward to upper aquifers and undergo chemical oxidation facilitated by the presence of Fe(III)-bearing minerals in the sediments. This process leads to the formation of elemental sulfur or thiosulfate. The occurrence of this reaction is supported by the lower $\delta^{34}$S values observed for elemental sulfur than for hydrogen sulfide in the FW sample from lower oil deposits [Fig. 2 (B)]. Previous studies have indicated the occurrence of chemical sulfide oxidation with metal oxides, such as FeOOH and magnetite (Fe$^{2+}$Fe$^{3+}$$_2$O$_4$), in marine sediments (Holmkvist et al., 2011; Bottrell et al., 2008). Given that FeOOH is more readily reduced than magnetite during sediment burial, resulting in the preservation of

340    magnetite (Canfield et al., 1992), magnetite likely serves as the primary agent responsible for sulfide oxidation at this study site. Despite the predominance of sulfur-reducing microorganisms in the upper aquifers as opposed to the absence of microbial cells in the lower oil deposits, the differences in $\delta^{34}S$ values of hydrogen sulfide and elemental sulfur are not substantial between the upper and lower locations. This suggests that biological dissimilatory sulfur reduction [Fig. 2 (C)] is much less important than chemical sulfide oxidation [(B)] with respect to its influence on $\delta^{34}S$, which should be linked to differences in

345    the sulfur flux of the biological and chemical processes in the upper aquifers.

A previous study indicated that the degree of generation of hydrogen sulfide from crude oil depends on various factors, including the concentration of sulfur compounds in the oil, oil biodegradation coupled with microbial sulfate reduction and oil densification during burial (Zhu et al., 2017). At the study site, the concentration of sulfur compounds in oil-source rocks, as represented by the sulfur-to-carbon atomic ratio (S/C), was relatively low, ranging from 0.011-0.049, with an average of 0.025

350    (Suzuki et al., 1995). For comparison, high-sulfur oils exhibit an S/C ratio greater than 0.06 (Orr, 1986). This implies a low level of upward migration of hydrogen sulfide from oil deposits to upper aquifers. Nevertheless, our findings indicate that the shifts in microbial population, diversity and function may be due to the chemical reactions induced by geothermal heating, which underscores the potential for a more dynamic chemical and microbial interactions that drives sulfur and carbon cycling in other deeply buried sedimentary environments.

355

*Data Availability.* DNA sequencing data are available at GenBank, as described in the Materials and Methods section. Other datasets generated during the current study are available in the manuscript, supplementary information or from the corresponding author upon reasonable request.

360    *Competing Interests.* The authors have no relevant financial or nonfinancial interests to disclose.

*Author Contributions.* All the authors contributed to the study conception and design. Taiki Katayama, Hideyoshi Yoshioka and Yasuaki Hanamura contributed to the study conception and design and collected the samples. Hideyoshi Yoshioka and Toshiro Yamanaka conducted water and sediment geochemical analyses. Taiki Katayama cultivated and analyzed the DNA.

365    Taiki Katayama, Hideyoshi Yoshioka and Susumu Sakata wrote the manuscript. All the authors have read and approved the final manuscript.

*Acknowledgments.* We acknowledge Toshitaka Araki of the JX Nippon Oil and Gas Exploration Corporation for sample collection. We thank Chiwaka Miyako, Fumie Nozawa and Hanako Mochimaru for assistance in sample collection, sequencing

370    analysis and cultivation experiments. We would like to thank Tatsuo Aono for his cooperation in the radiotracer experiments at the National Institute of Radiological Sciences (NIRS-QST). We would also like to thank Kazuya Morimoto for valuable comments regarding the chemical reactions of sulfur compounds and Takeshi Nakajima for managing this joint research project.

## References

375 Aloisi, G., Gloter, A., Krüger, M., Wallmann, K., Guyot, F., and Zuddas, P.: Nucleation of calcium carbonate on bacterial nanoglobules, Geology, 34, 1017-1020, 10.1130/g22986a.1, 2006.

Arndt, S., Jørgensen, B. B., LaRowe, D. E., Middelburg, J. J., Pancost, R. D., and Regnier, P.: Quantifying the degradation of organic matter in marine sediments: A review and synthesis, Earth-Sci Rev, 123, 53-86, https://doi.org/10.1016/j.earscirev.2013.02.008, 2013.

380 Bar-On, Y. M., Phillips, R., and Milo, R.: The biomass distribution on Earth, Proc Natl Acad Sci USA, 115, 6506-6511, doi:10.1073/pnas.1711842115, 2018.

Bottrell, S. H., Bottcher, M. E., Schippers, A., Parkes, R. J., Jorgensen, B. B., Raiswell, R., Telling, J., and Gehre, M.: Abiotic sulfide oxidation via manganese fuels the deep biosphere, Geochim Cosmochim Ac, 72, A102, https://doi.org/10.1016/j.gca.2008.05.005, 2008.

385 Buessecker, S., Chadwick, G. L., Quan, M. E., Hedlund, B. P., Dodsworth, J. A., and Dekas, A. E.: Mcr-dependent methanogenesis in *Archaeoglobaceae* enriched from a terrestrial hot spring, ISME J, 17, 1649-1659, 10.1038/s41396-023-01472-3, 2023.

Canfield, D. E., Raiswell, R., and Bottrell, S.: The reactivity of sedimentary iron minerals toward sulfide, Am J Sci, 292, 659-683, DOI 10.2475/ajs.292.9.659, 1992.

390 Clayton, R. N., Friedman, I., Graf, D. L., Mayeda, T. K., Meents, W. F., and Shimp, N. F.: The origin of saline formation waters: 1. Isotopic composition, J Geophys Res (1896-1977), 71, 3869-3882, https://doi.org/10.1029/JZ071i016p03869, 1966.

Conrad, R.: Complexity of temperature dependence in methanogenic microbial environments, Front Microbiol, 14, 10.3389/fmicb.2023.1232946, 2023.

Fredrickson, J. K., McKinley, J. P., Bjornstad, B. N., Long, P. E., Ringelberg, D. B., White, D. C., Krumholz, L. R., Suflita, J.

395 M., Colwell, F. S., Lehman, R. M., Phelps, T. J., and Onstott, T. C.: Pore-size constraints on the activity and survival of subsurface bacteria in a late Cretaceous shale-sandstone sequence, northwestern New Mexico, Geomicrobiol J, 14, 183-202, https://doi.org/10.1080/01490459709378043, 1997.

Fukano, T., Mizukami, T., Aoyama, T., and Maehara, Y.: Water saturation of natural gas dissolved in water sandstone and its interpretation, Nakajo oil and gas field, Japan, J Jpn Assoc Petrol Technol, 88, 408-418, 2023.

400 Gam, Z. B. A., Daumas, S., Casalot, L., Bartoli-Joseph, M., Necib, S., Linard, Y., and Labat, M.: *Thermanaeromonas burensis* sp. nov., a thermophilic anaerobe isolated from a subterranean clay environment, Int J Syst Evol Microbiol, 66, 445-449, https://doi.org/10.1099/ijsem.0.000739, 2016.

Hattori, S., Kamagata, Y., Hanada, S., and Shoun, H.: *Thermacetogenium phaeum* gen. nov., sp. nov., a strictly anaerobic, thermophilic, syntrophic acetate-oxidizing bacterium, Int J Syst Evol Microbiol, 50, 1601-1609,

405 https://doi.org/10.1099/00207713-50-4-1601, 2000.

Heuer, V. B., Inagaki, F., Morono, Y., Kubo, Y., Spivack, A. J., Viehweger, B., Treude, T., Beulig, F., Schubotz, F., Tonai, S., Bowden, S. A., Cramm, M., Henkel, S., Hirose, T., Homola, K., Hoshino, T., Ijiri, A., Imachi, H., Kamiya, N., Kaneko,

M., Lagostina, L., Manners, H., McClelland, H.-L., Metcalfe, K., Okutsu, N., Pan, D., Raudsepp, M. J., Sauvage, J., Tsang, M.-Y., Wang, D. T., Whitaker, E., Yamamoto, Y., Yang, K., Maeda, L., Adhikari, R. R., Glombitza, C., Hamada, Y.,

410    Kallmeyer, J., Wendt, J., Wörmer, L., Yamada, Y., Kinoshita, M., and Hinrichs, K.-U.: Temperature limits to deep subseafloor life in the Nankai Trough subduction zone, Science, 370, 1230-1234, 10.1126/science.abd7934, 2020.

Holmkvist, L., Ferdelman, T. G., and Jørgensen, B. B.: A cryptic sulfur cycle driven by iron in the methane zone of marine sediment (Aarhus Bay, Denmark), Geochim Cosmochim Ac, 75, 3581-3599, https://doi.org/10.1016/j.gca.2011.03.033, 2011.

Horsfield, B., Schenk, H. J., Zink, K., Ondrak, R., Dieckmann, V., Kallmeyer, J., Mangelsdorf, K., di Primio, R., Wilkes, H.,

415    Parkes, R. J., Fry, J., and Cragg, B.: Living microbial ecosystems within the active zone of catagenesis: Implications for feeding the deep biosphere, Earth Planet Sc Lett, 246, 55-69, https://doi.org/10.1016/j.epsl.2006.03.040, 2006.

Jørgensen, B. B. and Boetius, A.: Feast and famine — microbial life in the deep-sea bed, Nat Rev Microbiol, 5, 770-781, 10.1038/nrmicro1745, 2007.

Kaneko, K. and Igari, S.: Comopositional and carbon isotopic changes of natural gas through generation, migration and

420    accumulation processes, J Jpn Assoc Petrol Technol, 85, 62-73, 10.3720/japt.85.62, 2020.

Katayama, T., Yoshioka, H., Takahashi, H. A., Amo, M., Fujii, T., and Sakata, S.: Changes in microbial communities associated with gas hydrates in subseafloor sediments from the Nankai Trough, FEMS Microbiol Ecol, 92, 10.1093/femsec/fiw093, 2016.

Katayama, T., Yoshioka, H., Kaneko, M., Amo, M., Fujii, T., Takahashi, H. A., Yoshida, S., and Sakata, S.: Cultivation and

425    biogeochemical analyses reveal insights into methanogenesis in deep subseafloor sediment at a biogenic gas hydrate site, ISME J, 16, 1464-1472, 10.1038/s41396-021-01175-7, 2022.

Katayama, T., Yoshioka, H., Muramoto, Y., Usami, J., Fujiwara, K., Yoshida, S., Kamagata, Y., and Sakata, S.: Physicochemical impacts associated with natural gas development on methanogenesis in deep sand aquifers, ISME J, 9, 436-446, 10.1038/ismej.2014.140, 2015.

430    Katayama, T., Yoshioka, H., Yamanaka, T., Takeuchi, M., Muramoto, Y., Usami, J., Ikeda, H., and Sakata, S.: Microbial community structure in deep natural gas-bearing aquifers subjected to sulfate-containing fluid injection, J Biosci Bioeng, 127, 45-51, https://doi.org/10.1016/j.jbiosc.2018.06.013, 2019.

Katayama, T., Nobu, M. K., Kusada, H., Meng, X. Y., Hosogi, N., Uematsu, K., Yoshioka, H., Kamagata, Y., and Tamaki, H.: Isolation of a member of the candidate phylum 'Atribacteria' reveals a unique cell membrane structure, Nat Commun, 11,

435    6381, 10.1038/s41467-020-20149-5, 2020.

Kato, S.: Geochemistry of formation waters from oil and gas elds in Niigata Prefecture, Japan, J Jpn Assoc Petrol Technol, 83, 257-266, 10.3720/japt.83.257, 2018.

Kato, S. and Kajiwara, Y.: Isotopic composition of hydrogen and oxygen in waters associated with oil and gas from Niigata basin, Japan, J Jpn Assoc Petrol Technol, 51, 113-122, 10.3720/japt.51.113, 1986.

440    Katoh, K. and Standley, D. M.: MAFFT multiple sequence alignment software version 7: improvements in performance and usability, Mol Biol Evol, 30, 772-780, 10.1093/molbev/mst010, 2013.

Kobayashi, I.: Cenozoic strata of the Niigata region and the paleo-Sea of Japan, J Jpn Assoc Petrol Technol, 65, 305-313, 10.3720/japt.65.305, 2000.

Krumholz, L. R., McKinley, J. P., Ulrich, F. A., and Suflita, J. M.: Confined subsurface microbial communities in Cretaceous rock, Nature, 386, 64-66, Doi 10.1038/386064a0, 1997.

Kvenvolden, K. A.: A review of the geochemistry of methane in natural gas hydrate, Org Geochem, 23, 997-1008, Doi 10.1016/0146-6380(96)00002-2, 1995.

Larter, S. R. and Senftle, J. T.: Improved kerogen typing for petroleum source rock analysis, Nature, 318, 277-280, 10.1038/318277a0, 1985.

Liu, Y., Beer, L. L., and Whitman, W. B.: Sulfur metabolism in archaea reveals novel processes, Enviro Microbiol, 14, 2632-2644, https://doi.org/10.1111/j.1462-2920.2012.02783.x, 2012.

Lovley, D. R. and Chapelle, F. H.: Deep Subsurface Microbial Processes, Rev Geophys, 33, 365-381, 10.1029/95rg01305, 1995.

Luton, P. E., Wayne, J. M., Sharp, R. J., and Riley, P. W.: The *mcrA* gene as an alternative to 16S rRNA in the phylogenetic analysis of methanogen populations in landfill, Microbiology, 148, 3521-3530, 10.1099/00221287-148-11-3521, 2002.

Magnabosco, C., Lin, L. H., Dong, H., Bomberg, M., Ghiorse, W., Stan-Lotter, H., Pedersen, K., Kieft, T. L., van Heerden, E., and Onstott, T. C.: The biomass and biodiversity of the continental subsurface, Nat Geosci, 11, 707-717, 10.1038/s41561-018-0221-6, 2018.

Malinverno, A. and Martinez, E. A.: The effect of temperature on organic carbon degradation in marine sediments, Sci Rep, 5, 17861, 10.1038/srep17861, 2015.

Mcmahon, P. B. and Chapelle, F. H.: Microbial-Production of Organic-Acids in Aquitard Sediments and Its Role in Aquifer Geochemistry, Nature, 349, 233-235, Doi 10.1038/349233a0, 1991.

McMahon, S. and Parnell, J.: Weighing the deep continental biosphere, FEMS Microbiol Ecol, 87, 113-120, 10.1111/1574-6941.12196, 2014.

Mei, R., Kaneko, M., Imachi, H., and Nobu, M. K.: The origin and evolution of methanogenesis and Archaea are intertwined, PNAS Nexus, 2, 10.1093/pnasnexus/pgad023, 2023.

Middelburg, J. J.: A simple rate model for organic matter decomposition in marine sediments, Geochim Cosmochim Ac, 53, 1577-1581, https://doi.org/10.1016/0016-7037(89)90239-1, 1989.

Milkov, A. V. and Etiope, G.: Revised genetic diagrams for natural gases based on a global dataset of >20,000 samples, Org Geochem, 125, 109-120, https://doi.org/10.1016/j.orggeochem.2018.09.002, 2018.

Mori, K., Hanada, S., Maruyama, A., and Marumo, K.: *Thermanaeromonas toyohensis* gen. nov., sp. nov., a novel thermophilic anaerobe isolated from a subterranean vein in the Toyoha Mines, Int J Syst Evol Microbiol, 52, 1675-1680, https://doi.org/10.1099/00207713-52-5-1675, 2002.

Orr, W. L.: Kerogen/asphaltene/sulfur relationships in sulfur-rich Monterey oils, Org Geochem, 10, 499-516, https://doi.org/10.1016/0146-6380(86)90049-5, 1986.

Parkes, R. J., Cragg, B. A., and Wellsbury, P.: Recent studies on bacterial populations and processes in subseafloor sediments: A review, Hydrogeol J, 8, 11-28, Doi 10.1007/Pl00010971, 2000.

Parkes, R. J., Wellsbury, P., Mather, I. D., Cobb, S. J., Cragg, B. A., Hornibrook, E. R. C., and Horsfield, B.: Temperature activation of organic matter and minerals during burial has the potential to sustain the deep biosphere over geological timescales, Org Geochem, 38, 845-852, https://doi.org/10.1016/j.orggeochem.2006.12.011, 2007.

Pruesse, E., Quast, C., Knittel, K., Fuchs, B. M., Ludwig, W., Peplies, J., and Glockner, F. O.: SILVA: a comprehensive online resource for quality checked and aligned ribosomal RNA sequence data compatible with ARB, Nucleic Acids Res, 35, 7188-7196, 10.1093/nar/gkm864, 2007.

Schippers, A., Neretin, L. N., Kallmeyer, J., Ferdelman, T. G., Cragg, B. A., John Parkes, R., and Jørgensen, B. B.: Prokaryotic cells of the deep sub-seafloor biosphere identified as living bacteria, Nature, 433, 861-864, 10.1038/nature03302, 2005.

Slobodkina, G. B., Kolganova, T. V., Chernyh, N. A., Querellou, J., Bonch-Osmolovskaya, E. A., and Slobodkin, A. I.: *Deferribacter autotrophicus* sp. nov., an iron(III)-reducing bacterium from a deep-sea hydrothermal vent, Int J Syst Evol Microbiol, 59, 1508-1512, https://doi.org/10.1099/ijs.0.006767-0, 2009.

Suzuki, N., Sampei, Y., and Matsubayashi, H.: Organic geochemical difference between source rocks from Akita and Niigata oil fields, Neogene Tertiary, Japan, J Jpn Assoc Petrol Technol, 60, 62-75, 10.3720/japt.60.62, 1995.

Takai, K., Kobayashi, H., Nealson, K. H., and Horikoshi, K.: *Deferribacter desulfuricans* sp. nov., a novel sulfur-, nitrate- and arsenate-reducing thermophile isolated from a deep-sea hydrothermal vent, Int J Syst Evol Microbiol, 53, 839-846, 10.1099/ijs.0.02479-0, 2003.

Takano, O., Moriya, S., Nishimura, M., Akiba, F., Abe, M., and Yanagimoto, Y.: Sequence stratigraphy and characteristics of depositional systems of the Upper Miocene to Lower Pleistocene in the Kitakambara Area, Niigata Basin, central Japan, Jour Geol Soc Japan, 107, 585-604, 10.5575/geosoc.107.585, 2001.

van de Meent, D., Brown, S. C., Philp, R. P., and Simoneit, B. R. T.: Pyrolysis-high resolution gas chromatography and pyrolysis gas chromatography-mass spectrometry of kerogens and kerogen precursors, Geochim Cosmochim Ac, 44, 999-1013, https://doi.org/10.1016/0016-7037(80)90288-4, 1980.

Vinson, D. S., Blair, N. E., Martini, A. M., Larter, S., Orem, W. H., and McIntosh, J. C.: Microbial methane from in situ biodegradation of coal and shale: A review and reevaluation of hydrogen and carbon isotope signatures, Chem Geol, 453, 128-145, https://doi.org/10.1016/j.chemgeo.2017.01.027, 2017.

Vítězová, M., Lochman, J., Zapletalová, M., Ratering, S., Schnell, S., and Vítěz, T.: Archaeal community dynamics in biogas fermentation at various temperatures assessed by *mcrA* amplicon sequencing using different primer pairs, World J Microbiol Biotechnol, 37, 188, 10.1007/s11274-021-03152-w, 2021.

Waseda, S. and Nakai, N.: Isotopic compositions of meteoric and surface waters in Central and Northeast Japan, Chikyukagaku, 17, 83-91, 10.14934/chikyukagaku.17.83, 1983.

Yamanaka, T., Maeto, K., Akashi, H., Ishibashi, J. I., Miyoshi, Y., Okamura, K., Noguchi, T., Kuwahara, Y., Toki, T., Tsunogai, U., Ura, T., Nakatani, T., Maki, T., Kubokawa, K., and Chiba, H.: Shallow submarine hydrothermal activity with

510     significant contribution of magmatic water producing talc chimneys in the Wakamiko Crater of Kagoshima Bay, southern Kyushu, Japan, J Volcanol Geoth Res, 258, 74-84, Doi 10.1016/J.Jvolgeores.2013.04.007, 2013.

Yang, S., Liebner, S., Alawi, M., Ebenhöh, O., and Wagner, D.: Taxonomic database and cut-off value for processing *mcrA* gene 454 pyrosequencing data by MOTHUR, J Microbiol Methods, 103, 3-5, https://doi.org/10.1016/j.mimet.2014.05.006, 2014.

515     Zhu, G., Liu, X., Yang, H., Su, J., Zhu, Y., Wang, Y., and Sun, C.: Genesis and distribution of hydrogen sulfide in deep heavy oil of the Halahatang area in the Tarim Basin, China, J Nat Gas Geosci, 2, 57-71, https://doi.org/10.1016/j.jnggs.2017.03.004, 2017.